

Full-scale measurement and analysis of train slipstreams and wakes

Baker, C. J.; Quinn, A.; Sima, M.; Hoefener, L.; Licciardello, R.

DOI:

[10.1177/0954409713485944](https://doi.org/10.1177/0954409713485944)

License:

Creative Commons: Attribution-NonCommercial-NoDerivs (CC BY-NC-ND)

Document Version

Peer reviewed version

Citation for published version (Harvard):

Baker, CJ, Quinn, A, Sima, M, Hoefener, L & Licciardello, R 2013, 'Full-scale measurement and analysis of train slipstreams and wakes: Part 1 Ensemble averages', *Proceedings of the Institution of Mechanical Engineers Part F Journal of Rail and Rapid Transit*, vol. 228, no. 5, pp. 451-467. <https://doi.org/10.1177/0954409713485944>

[Link to publication on Research at Birmingham portal](#)

Publisher Rights Statement:

This is an Author's Original Manuscript of an article submitted for consideration in the Proc IMechE Part F: J Rail and Rapid Transit 2014, 0(0) 1–17 Copyright: IMechE 2012 Reprints and permissions: sagepub.co.uk/journalsPermissions.nav DOI: DOI: 10.1177/0954409713485944 pif.sagepub.com

General rights

Unless a licence is specified above, all rights (including copyright and moral rights) in this document are retained by the authors and/or the copyright holders. The express permission of the copyright holder must be obtained for any use of this material other than for purposes permitted by law.

- Users may freely distribute the URL that is used to identify this publication.
- Users may download and/or print one copy of the publication from the University of Birmingham research portal for the purpose of private study or non-commercial research.
- User may use extracts from the document in line with the concept of 'fair dealing' under the Copyright, Designs and Patents Act 1988 (?)
- Users may not further distribute the material nor use it for the purposes of commercial gain.

Where a licence is displayed above, please note the terms and conditions of the licence govern your use of this document.

When citing, please reference the published version.

Take down policy

While the University of Birmingham exercises care and attention in making items available there are rare occasions when an item has been uploaded in error or has been deemed to be commercially or otherwise sensitive.

If you believe that this is the case for this document, please contact UBIRA@lists.bham.ac.uk providing details and we will remove access to the work immediately and investigate.

Full scale measurement and analysis of train slipstreams and wakes: Part 1 Ensemble averages

C J Baker, Andrew Quinn

Birmingham Centre for Railway Research and Education, University of Birmingham

M Sima

Bombardier Transportation, Sweden

L Hoefener

Deutsche Bahn AG, DB Systemtechnik, Germany

R Licciardello

Sapienza Università di Roma, Italy

Abstract

This paper describes a series of extensive and unique full scale measurements of the slipstreams of trains of various types that were carried out as part of the EU sponsored AeroTRAIN project, together with the analysis of the experimental data. These experiments were carried out with the fundamental aim of seeking to reduce the complexity of the current TSI testing methodology. Experimental sites in Spain and Germany were used, for a range of different train types – high speed single unit trains, high speed double unit trains, conventional passenger units and locomotive / coach combinations. The data that was obtained was supplemented by other data from previous projects. The analysis primarily involved a study of the ensemble averages of the slipstream velocities, measured both at trackside and above platforms. The differences between the flows around different train types were elucidated, and the effect of platforms on slipstream behaviour described. A brief analysis of the effects of cross winds on slipstream behaviour was also carried out. Through a detailed analysis of slipstream velocity components, the detailed nature of the flow around the nose and in the near wake of the train was investigated, again revealing differences in flow pattern between different trains. Significant similarity in the far wake flows was revealed. These fundamental results form the basis for the detailed discussion of the proposed TSI methodology that will be presented in Part 2 of this paper. Overall the results enable the nature of the flow field around trains to be understood in far greater detail than before, and also allow the developments of a revised TSI methodology which is more efficient than current practice.

Notation

U	Ensemble mean of horizontal slipstream velocity, normalised by train speed
u	Ensemble mean of longitudinal slipstream velocity, normalised by train speed
v	Ensemble mean of lateral slipstream velocity, normalised by train speed
X	Distance from the end of the train
x	Distance along the track (measured from vehicle front)
y	Distance normal to the track (measured from the centre of the track)
y'	Distance normal to the track (measured from the nearest rail)
z	Distance in the vertical direction (measured from the top of the rail)

1. Introduction

The flow around high speed trains has been described in detail in [1], and in that paper the nature of the boundary layer development along the side of the train and in the wake behind the train, (as a whole referred to colloquially as the train slipstream), is described in some detail. The flow can be divided into a number of regions along the train – the nose region, which is dominated by large, inviscid pressure and velocity transients; the boundary layer region, in which a highly disturbed and non-equilibrium turbulent boundary layer grows along the side of the train and on the train roof; a near wake region which is dominated by large scale unsteady flow structures; and a far wake region that exhibits a gradual decrease in slipstream velocities away from the train. These trends are illustrated in figure 1, (taken from [2]), which shows an ensemble average of non-dimensional slipstream velocity measurements from a number of train passes (i.e. the average of a number of individual runs) for the German Railways (DB) ICE-1 train. Note that the x axis is the distance from the nose of the train – which is equivalent to the velocity multiplied by the time after the train nose passes a particular point. It can be seen that the highest slipstream velocities are found in the train wake (around 400m from the train nose – the train is 364m long), and this observation seems to have some generality for high speed passenger trains, although not necessarily for other types of train. At this point it is worth mentioning that the slipstream velocity time histories from individual runs are highly variable, (as would be expected, since they are dominated by large scale turbulent flows), and thus the technique of ensemble averaging is required in order to be able to interpret them [2].

Knowledge of the magnitudes of velocities and pressures in the slipstream of a train is important for a number of reasons – high pressure transients can cause large, transient loads on trackside and station structures and on passing trains. High slipstream velocities can result in dangerous conditions for passengers waiting on platforms and for workers at the trackside, and can cause objects such as push chairs to move. These effects thus need to be taken into account in the development and authorisation of new trains. A consideration of these effects, as well as other aerodynamic issues, has led to the development of a series of standards on train aerodynamics [3], material from which has been incorporated into the Technical Specifications for Interoperability (TSI), giving limiting values for slipstream velocities. These are being developed to allow trains to run across national boundaries in Europe. The TSI methodology for the assessment of slipstream velocities [4] is based on a method outlined in [3] for assessing

the magnitude of the slipstreams of a train and requires that full scale measurements be made at specific points on a platform and at the trackside for 20 train passes within defined vehicle speed ranges, for low wind speed conditions only. The maximum one second moving average velocity for each train pass is then calculated. A value of the mean plus two standard deviations of the ensemble of one second values is then compared with limiting values specified by the TSI. The need for two measurement locations, one at trackside and one on a platform, makes this type of testing somewhat cumbersome, particularly accessing the required platform test site. A method based on one set of measurements at the trackside that is transferable to any country would be rather more convenient and cost-effective. For this reason, a work package of the recent EU sponsored project AeroTRAIN (part of the larger TrioTRAIN cluster of projects – see http://www.triotrain.eu/TRIO_generalbackground.htm) was devoted to looking at the testing procedure for slipstream measurements, with a view to reducing the number of measurement locations. This work involves the following aspects.

- The collation of existing slipstream data from earlier projects – specifically material from the RAPIDE project [5] and material from UK tests carried out in the 1980s and 1990s [6].
- Measurement campaigns on lines in Spain and Germany, to measure the slipstreams for a variety of high speed train and conventional train types at trackside and above platforms.
- The analysis of the data to determine a possible revised TSI methodology with a simplified test procedure, to identify the magnitudes of slipstreams from different vehicles, and to develop a methodology to assess single vehicles within trains with respect to their relevance / impact on the slipstream effects of a particular train configuration.

This paper is the first part of a two part study that will present and analyse the results of this work. In this paper (Part 1) attention will be focussed on the ensemble averages of slipstream velocities for a wide variety of trains. The experimental set up is described in section 2, and the technique of ensemble averaging is described. The ensemble averages are considered for trackside and platform cases in sections 3 and 4, and the effect of cross winds is considered in section 5. Section 6 discusses the results in some detail, and elucidates some of the flow phenomena found in train boundary layers and wakes. Finally conclusions are drawn in section 7. Part 2 of this paper will go on to consider the gust values that were measured, again for a wide variety of trains, and how these

values relate to those in the current TSI methodology. The rationale behind a proposed new measurement procedure will then be outlined.

2. Experimental methodology

2.1 The experimental sites and trains

For the full scale experiments, three experimental sites were used in Spain and Germany. The experimental conditions, anemometer positions, train types etc are summarised in table 1, satellite and surface photographs of the sites are shown in figure 2, and photographs of the different train types are shown in figure 3. These sites can be briefly described as follows.

- Tests in Spain on both tracks of the Madrid / Barcelona 300 kph high speed line near Guadalajara – Yebes railway station (denoted in what follows by GY) by Deutsche Bahn (DB) on track 1 (the Barcelona direction) and track 2 (the Madrid direction), and by Bombardier Transportation (BT) on track 1 only. The measurements were made on straight track on a level section of exposed ground, at the transition between a shallow cutting and an embankment. Measurements were made at the trackside for a number of different high speed train types operated by RENFE running at up to 300kph - S-100 (Alstom, derived from the TGV) single units; S-102 (Talgo-Bombardier) in both single and multiple unit configurations; S-103 (Siemens, related to the DB ICE-3, known as the Velaro) again in both single and multiple unit configurations; the S-120 (CAF) single unit; and the S-130 (Talgo-Bombardier) single unit. In addition measurements were made for the S-252 locomotive followed by a rake of Talgo coaches. Note that these experiments also measured a variety of other aerodynamic phenomena as part of the AeroTRAIN project (pressure transients, track bed pressures etc), but these will not be considered further here.
- Tests in Germany at Westendorf station (denoted by WE), by DB on track 1 and platform 1 (0.18m high above top of rail) (Donauwörth to Augsburg direction) and the University of Birmingham (UB) on track 2 and platform 2 (0.38m high) (Augsburg to Donauwörth direction). The trackside sites were on straight track on exposed level terrain, whilst the platform sites were necessarily somewhat more enclosed. Measurements were made on two types of DB high speed train (although limited to 200kph for the current measurements) – double unit ICE-2's, and single unit ICE-T trains. In addition measurements were made on the DB BR440 short passenger unit and the DOSTO double deck train, either pushed or pulled by a

BR111 locomotive. Again a variety of other aerodynamic phenomena were measured in the same experiments.

- Tests in Germany at Kutzenhausen station (denoted by KH) by UB on the 0.38m high platform in the Ulm direction. The site was enclosed by station fencing and trees, and was on a gently curving section of track. Measurements were made of the slipstreams of the ICE-1 and ICE-3 high speed trains (again limited to 200kph on this stretch of line) and of the DB BR101 locomotive pulling a rake of carriages.

In the analysis that is described in this paper data has also been used from the following two previous investigations.

- The RAPIDE project [5]. This project studied a number of different aerodynamic effects, including detailed measurements of train slipstreams. In this paper the data that was obtained for a 14 car ICE-1, at trackside and platform locations, and a single unit ICE-2 at a trackside location will be used.
- A variety of measurements made in the UK in the 1990's and reported in [6]. Most of these measurements were for only a small number of train passes. However some data for multiple passes was obtained for a Class 91 locomotive pulling a rake of carriages, at trackside and platform locations, and this data will be used in the analysis that follows.

2.2 Instrumentation

The measurements that were made primarily used ultra-sonic anemometers of various sorts, mounted at the positions outlined in table 1. The DB measurements were made using 2D anemometers that measured only the two components of horizontal velocity whilst the BT and UB measurements were made using 3D anemometers that also gave information on the vertical velocity. The measured vertical velocity components were however always small and only horizontal velocities will be presented in what follows. Measurement uncertainties are below $\pm 3\%$, which it will be seen are an order of magnitude smaller than the uncertainties associated with the unsteady, turbulent nature of the measured slipstream velocities. Ambient wind velocities and directions were obtained from the anemometers positioned at 0.2m above the track (or, where there were only platform based measurements, from a

reference anemometer place away from the track) for a 3s period before each train pass (the TSI recommended methodology [4]). Train velocities were measured using light gates mounted to the track by DB and BT whilst the UB results were obtained by measuring the lag between the train nose pressure peaks at two anemometer measurement stations.

2.3 Ensemble analysis

In this paper, the basic analytical technique that will be used is that of ensemble averaging. In this process a number of runs were selected for each train type that had consistent train speeds (usually near the maximum operating speed for a particular train type) and for which the ambient wind speed was low (always less than the 2m/s specified in [4] and for some ensembles, less than 1m/s). The time base for each run was then transformed into a distance from the passing of the train nose, and the measured slipstream velocities were normalised by train speed. The time histories were then aligned, with $x=0$ as either the position of the first light gate (DB, BT) or as the position of the nose pressure peak(UB), and an average and standard deviation of the results found at (usually) 1m increments in distance from 200m before the train nose to 800m behind the train nose. These are referred to in what follows as the ensemble mean and standard deviation. A typical example for the S-103 data is shown in figure 4 below, showing the results for normalised slipstream velocity for 10 individual runs, together with the ensemble mean and the mean \pm the standard deviation. The very large run to run variation is apparent, with very large fluctuations in the near wake of the train. Similar trends were observed in earlier work – see [2] for example. It was found that around 20 train runs were ideally required to obtain accurate ensemble averages, but this was not possible in a number of cases. The issue of accuracy and uncertainty in the experimental data will be discussed at length in Part 2 of this paper. Table 2 shows the data for which ensemble averages were obtained and the number of train runs used in each case. It will be seen that for some trains the number of runs is less than the ideal value of 20. This needs to be borne in mind in what follows. Note that ensemble analysis was not carried out for all the cases shown in table 1 – some datasets were not suitable for this type of analysis, but will be used in the gust analysis in Part 2 of this paper.

3. Ensemble analysis of trackside experimental data

The data from the trackside experiments described in the last section were used to obtain ensemble averages for the horizontal slipstream velocity, for all train types for which sufficient data existed. All data for which the TSI wind speed limit of 2m/s was exceeded were excluded. The number of runs in each ensemble is shown in table 2 – in general 20 runs were used if possible, but for some trains this number was significantly reduced. The slipstream velocities at 1m distances along the trains were obtained from a re-sampling of the original data, the data aligned using the light gate signal as the first axle of the train passed (for the DB and BT data) or the position of the nose pressure peak (for the UB data), and the ensemble mean and standard deviations calculated. These are then normalised by dividing by the train velocity to give the ensemble means and standard deviations presented here. The results for the mean values are shown in figures 5 to 8 for high speed single unit trains, high speed double unit trains, multiple units and locomotive plus coaches respectively. The ensembles are aligned such that the train nose passes at $x=0$. The location of the rear of the train is marked on each figure. We will consider each of these figures in turn.

Figure 5 shows the ensemble averages for a variety of high speed trains. We begin with figures 5 a and b which show the results of two nominally identical sets of measurements on different tracks in the Spanish (GY) experiments for the S-103, the T12 experiments being carried out by DB and the T1 experiments being carried out by BT. Figure 5a shows data for two anemometer heights of 0.2m and 1.2m whilst figure 5b shows data for three heights of 0.2m, 1.2m and 1.58m. The results are consistent with one another, with the difference between them being an indication of the differences that one might expect from one 20 run ensemble to another. The sharp nose peak can be seen, followed by an increase in slipstream velocity as the boundary layer along the train grows exposing the anemometers to higher slipstream velocities. This increase in velocity continues into the near wake (with very high ensemble standard deviations – not shown here), peaking around 50 to 100m behind the train, and then decaying gradually with distance. In general the slipstream velocity decreases with measurement height, showing the major effect of bogie roughness on the slipstream magnitudes. Figures 5c to 5i show similar figures for

a variety of other high speed single unit train types. They all possess similar overall characteristics, although for some trains there is a sharp increase in ensemble mean just behind the train. On close examination it would appear that trains with the more rounded noses / tails (S-100, S-103, ICE-T) show a more gradual rise in ensemble mean in the wake than those with less rounded noses / tails (S-120, S-130, ICE-1 and ICE-2 in single unit configuration—see the train photographs in figure 3) – show a much steeper rise in the wake. In general for all trains the slipstream magnitudes decrease with measurement height. The $z=0.2\text{m}$ values for the S-100 are particularly large relative to the values on that train at $z=1.2\text{m}$, perhaps reflecting the bogie configuration for this vehicle or due to the sloping wedge like front.

Figure 6 shows the slipstreams for a double unit ICE-2 train, at two tracks for the Westendorf experiments. The form of the ensemble mean can be seen to be very different to those in figure 5, with large peaks behind the junction between the two sets (where there is a major geometric discontinuity) and in the near wake. There can however be seen to be a distinct difference between the two sets of results, particularly for the $z=0.2\text{m}$ values on tracks 1 and 2. The reason for this is not immediately clear, but it should be noted that the number of runs for the T1 ensemble was small (table 3) and it may simply be that the observed differences reflect the fact that the data available was not fully able to describe the ensemble in a consistent fashion.

Figure 7 shows the ensemble means for a short multiple unit. Again many of the comments made above apply, with the nose peak, boundary layer growth and wake peak being clearly visible. Because of the shorter lengths of these trains in comparison with those shown in figure 5, the boundary layer growth is less, and this seems to lead to a rather abrupt increase in slipstream velocity in the near wake. This is also seen for the short S-120 in figure 5e.

Finally figure 8 shows the ensemble means for locomotives with trailing coaches. These can be seen to be very different from the high speed single unit train results of figure 5. Figure 8a, for the S-252 locomotive and trailing coaches, shows a significant peak around the locomotive. The wake peak in this case is not so obvious. For the Class 91 configuration in figure 8b, this peak around the locomotive can still be seen, although in this case the wake peak is larger. For this configuration, there was a driving trailer at the end of the train, of similar geometry to the Class 91, and the relatively sharp edged nature of this vehicle results in the strong wake peak of the type seen

for some of the high speed train single units. Figure 8c shows the DOSTO train being hauled by a BR111 locomotive, where there is a very sharp discontinuity in train shape. Here there can be seen to be large ensemble peaks both after the locomotive and in the wake. By contrast figure 8d, with the locomotive trailing only shows a wake peak. The maximum peak is lower for the loco trailing case than for the loco leading case. Obviously, the differences in cross section between locos and coaches has a significant effect on the shape of the slip stream pattern. The S-252 cross section slightly exceeds that of the trailing Talgo coaches, while the DOSTO coaches have the largest cross section of all studied vehicles. Thus the step in cross section on the consecutive coupling section can be expected to have different implication for the resulting slipstream.

4. The effect of platforms on slipstreams

Figure 9 shows a comparison between the ensembles measured on two different height platforms (0.18m and 0.38m) for three different types of train – the ICE-T high speed single unit, the ICE-2 high speed double unit and the BR440 short passenger unit. For all these trains the form of the ensembles is basically the same as those measured at trackside. However it can be seen that for the ICE-T and ICE-2 the magnitudes of the slipstreams is higher on the lower platform, particularly for the lower heights measured. This is possibly because the flow is forced onto the platform for the lower platform heights rather than being modified and attenuated in some way for the higher platform. Indeed a comparison of the ICE-T results with the trackside results of figure 5, and the ICE-2 results with the trackside results of figure 6, shows that the $z=1.2\text{m}$ velocities above the platform are very similar to the $z=0.2\text{m}$ velocities above the track for the lower platform height.

Figure 10 shows the results for the DOSTO short passenger unit, with the locomotive leading and trailing above the 0.18m platform. No data was available for these trains above the 0.38m platform. The difference between the locomotive leading and the locomotive trailing cases is very similar to that shown in figure 8. Again the magnitudes of the velocities at the lower measurement positions on the platform are similar to the lower measurement heights in the trackside measurements (figure 8), again suggesting that the flow near the ground is forced up onto the platform for this platform height.

Figure 11 shows ensembles for two sets of platform measurements from earlier investigations, for the ICE-1 above a 0.31m platform, and the Class 90 plus coaches above a 0.9m platform. For the ICE-1 results, a comparison with the results of figure 5 shows that the platform results are lower than those measured at trackside, probably because of the greater measurement height, but the form is essentially the same. For the Class 90 results a comparison can be made with the results of figure 8. Again the form of the ensemble is similar, although the platform velocities are significantly less than the trackside velocities, due to the increased measurement height and possibly the shielding effect of the 0.9m platform.

The results show a noticeable effect of the platform height on the measured slipstream velocities, which depends on the train shape and induced flow pattern. For some trains there is an amplification of the slipstream on the lowest platform height 0.18m. Above the 0.38m platform the velocities are similar to those at the trackside whereas above the 0.9m platform they are significantly attenuated. In this context it should be noted that also the 0.38m platform is a low platform, as the TSI specifies two platform heights, 0.55m and 0.76m.

5. Effect of wind on slipstreams

The effects of cross winds on slipstream magnitudes were investigated for the S-103 where a sufficient number of runs were available to be able to derive ensembles for different cross wind ranges (around 300 separate runs). For this analysis the TSI cross wind limit was not applied, and thus cross winds of up to 4m/s were used. The cross wind was defined by the yaw angle – the relative angle between the train and the wind, which combines in a useful way the cross wind velocity and the cross wind angle relative to the track. The data was split into three ranges; -1.5 to -0.5°, -0.5 to 0.5° and 0.5 to 1.5°. Ensembles were formed from 20 runs in each range i.e. for more train passages than were used in the analysis outlined in table 2. The results are shown in figure 12 for two measurement heights. It can be seen that the magnitudes of the peaks for negative yaw angles are significantly greater than for the positive yaw angles – for example the ensemble peaks for the measurements made at 1.2m height are around 0.07 for the positive yaw angles and 0.12 for the negative yaw angles. For the negative angles, the wake will be convected onto the measurement instruments by a cross wind and thus the results are as expected. (At this point it is worth noting that this data has already been described in [7], where an analysis was made of the cross wind performance of other train types. In these cases, the ensembles in the different yaw angle ranges were small and consisted of train passes with a large variation in vehicle speed, and are thus not as reliable as the S-103 data. The effect of cross winds for these vehicles was not clear cut, and in view of the limitations of the data, these are not considered further here. However, it does suggest there is an influence of the train shape and may therefore vary between trains.

6. Discussion

Figure 13 shows the trackside slipstream ensembles for three trains of different types – the S-102 (with a somewhat “pointed” nose and tail), the S-103 (with more rounded nose and tail) and the blunt S252 plus coaches. The plots show ensemble means for the along track velocity (u), the lateral velocity (v) and overall horizontal velocity (U). Plotted in this way the results are very revealing. Consider first the nose region. It is clear that for all the train types shown, there is a positive u component peak, followed by a negative peak, together with a positive v component peak (in the direction away from the train). This is shown more clearly for the S-103 in the expanded view of figure 14. In all cases, the total velocity peak in this region is largely determined by the magnitude of the lateral velocity peak. The shape of the u component largely mirrors the shape of the nose pressure transient (reported in [8] for example), as would be expected if the flow were inviscid. After the nose region, the boundary layer development is very different for the different types of train. For the S-102, the measuring point clearly lies outside the boundary layer for most of the train length, and thus the boundary layer growth is small, and the layer relatively thin even at the end of the train. For the S-103, the situation is somewhat different, with the measuring probes being immersed in the boundary layer for much of train length and showing an increasing velocity along the length of the train. In contrast to the S-103 which has two bogies with protruding dampers surrounding each inter car gap, the S-102 has no bogies but single axles located in the intercar gap and thus the gaps are much less accentuated. Moreover, the total number of axles is lower for the S-102. Therefore the growth of the boundary layer thickness, which is related to the roughness seen by the flow along the train, is slower for the S-102. The S-252 is very different again in this regard, with the bluff shape, and the discontinuity between the locomotive and the trailing coaches, resulting in a very rapid boundary layer development around the front of the train, with little resulting boundary layer development. Similar differences are observable in the near wake regions of the train. For the S-102, there is a very rapid increase in longitudinal velocity in the rear of the train, accompanied by a small negative lateral velocity pulse. This can be attributed to longitudinal vortex systems in the train wake - see for example [9]. For the S-103 by contrast, there is little increase in longitudinal velocity, and a rather larger lateral velocity peak. At this point the point made in [2] should be noted – because of the transient nature of the flow, the use of ensemble averaging in the near wake can produce erroneous results, with a smearing of significant velocity transients that only occur for a

proportion of the train passes, and that care is required in the interpretation of the ensemble averages in this region. For the S-252, the transition between boundary layer and wake regions is barely visible, although there is perhaps a negative lateral velocity transient. In the far wake the ensembles for all trains show a level of similarity - this will be explored further in what follows.

Now let us return to consideration of the nose region. The size of the ensemble nose peak will, in principle reflect the “bluntness” or otherwise of the train nose shape. Thus these peak magnitudes are shown in table 3 for a range of different types of train. The magnitudes are the measured magnitudes of the total horizontal velocity peak minus the average value before the train pass (caused by ambient wind conditions). This data divides essentially into two – values of around 0.05 to 0.07 for “streamlined” trains, and values of around twice this value for blunt trains. Within these categories, it is possible to distinguish some difference between trains – for example the nose peak for the S102 is somewhat less than that for the S-103 as might be expected from the above discussion.

The apparent similarity between the far wake flows for different vehicles has been noted above. To test this further a power law of the type

$$U = a(X)^n$$

was fitted to the ensemble velocities in the far wake for a variety of different types of train i.e. to the average wake velocities across a number of runs. X is here the distance from the end of the train. The far wake was taken to occur at distances greater than 100m from the end of the train. A typical curve fit for the S-103 ensemble average velocities is shown in figure 15 – it can be seen to be a close match to the data, as indeed it was for all the cases, except the $z=1.2\text{m}$ ensemble for the S100. The values of the best fit exponents are also shown in table 3. It can be seen that they are all very similar, and close to a value of 0.5. Now Baker [10], drawing on the work of Eskridge and Hunt [11], derived a formula for the decay of the wake of short road vehicles, that for a fixed point in the wake can be written in the notation of this paper as

$$U = \frac{b}{X} e^{-c/X^{0.5}}$$

where b and c are constants. This formula gives a more rapid wake velocity decay than was observed in these experiments. This is probably due to the fact that the formulation of Eskridge and Hunt was based on a short vehicle with form drag only, and boundary layer effects were not taken into account.

7. Conclusions

From the results that have been presented above the following major conclusions can be drawn.

1. The technique of ensemble averaging applied to the wide range of full scale results that were available have revealed a large amount of fundamental information concerning the flow field around a variety of different types of train.
2. For high speed trains, distinct difference in the flow field can be observed that seem to be dependent upon the nose / tail shape. “Pointed” noses seem to result in a thinner boundary layer along the lower train side, and a sharp increase in slipstream velocity in the near wake. More rounded train noses result in a more rapid boundary layer development, but a less vigorous flow in the near wake of the train. Moreover, the shape of the inter car gaps and the configuration of the bogies seem to have an additional influence.
3. For trains composed of two units, the discontinuity between them results in a peak in slipstream velocities around this discontinuity.
4. Locomotive / coach combinations have a very different type of slipstream ensemble, with high peaks around the nose of the locomotive and any discontinuity between the locomotive and the coaches. There is some indication that the locomotive leading case produces higher slipstream velocities than the locomotive trailing case, but this is based on only the small DOSTO dataset.
5. The effect of platforms on the nature of the slipstream velocities varies with platform height. For some kind of train, very low platforms can funnel the energetic low level flow onto the platform resulting in increased velocities. Higher platform heights can effectively block such flows and restrict them to below the platform height.
6. Where there is sufficient data available, a marked effect of cross winds on the slipstream ensembles can be observed, with the wake being convected onto the measurement position for some yaw angles. However, the effect on the TSI-compliant post processing remains minor due to the stochastic nature of the slipstreams.

7. A detailed analysis of the slipstream velocity components shows that the nose peak is primarily caused by lateral flow variations, with the longitudinal flows exhibiting reverse flows. In the near wake the more pointed trains show a strong longitudinal velocity component, presumably associated with the formation of longitudinal vortex structures, whilst the more rounded nose and tail shapes show a negative lateral velocity peak (directed to the track centre line). In the far wake, there is a surprising degree of similarity between almost all the data measured, with a slipstream velocity decay proportional to the square root of distance behind the train.

References

- [1] Baker, C.J.. The flow around high speed trains. *Journal of Wind Engineering and Industrial Aerodynamics*. 98, 277-298, 2010
- [2] Sterling M., Baker C.J., Jordan S.C., Johnson T., A study of the slipstreams of high speed passenger trains and freight trains, *Proc. Institute of Mechanical Engineers Part F: Journal of Rail and Rapid Transport*. 222, 177-19, 2008
- [3] CEN Railway applications — Aerodynamics — Part 4: Requirements and test procedures for aerodynamics on open track, CEN EN 14067-4:2005+A1, 2009
- [4] EU Technical Specification For Interoperability Relating to the ‘Rolling Stock’ Sub-System of the Trans-European High-Speed Rail System (HS RST TSI), 2008/232/EC, 2008
- [5] Schulte-Werning B., Matschke G., Grégoire R., Johnson, T., Rapide: A Project of Joint Railway Research of the European High-Speed Rail Operators. *World Congress on Railway Research WCRR’99 Tokyo, Japan, 1999*
- [6] Figura-Hardy G. I., Effective management of risk from slipstream effects at trackside and platforms. Appendix B. Analysis of existing experimental data on train slipstreams including the effects on pushchairs. RSSB project T425, 2005 http://www.rssb.co.uk/SiteCollectionDocuments/pdf/reports/research/T425_appb_final.pdf
- [7] Quinn A, Baker C, Sterling M, Sima M, Weise M, Hoefener L, Eisenlauer M The effect of cross winds on the slipstreams of high speed trains, *Proceedings 13th International Conference on Wind Engineering*, Amsterdam, 2011
- [8] Baker C, Jordan S, Gilbert T, Quinn A, Sterling M, Johnson T, Lane J, Transient aerodynamic pressures and forces on trackside and overhead structures due to passing trains. Part 1 Model scale experiments, Part 2 Code applications. To be submitted to *Journal of Rail and Rapid Transit*
- [9] C J Baker, S J Dalley, T Johnson, A Quinn, N G Wright, The slipstream and wake of a high speed train, *Proceedings of the Institution of Mechanical Engineers F Journal of Rail and Rapid Transit*, 215, 83-99, 2001
- [10] C J Baker, Flow and dispersion in vehicle wakes, *Journal of Fluids and Structures* 15, 7, 1031-1060, 2001
- [11] Eskridge R E, Hunt J C R (1979) Highway modelling part 1: Prediction of velocity and turbulence fields in the wakes of vehicles. *Journal of Applied Meteorology* 18, 387-400, 1979

Acknowledgements

This work was carried out as Work Package 5 of the EU FP7 AeroTRAIN project.

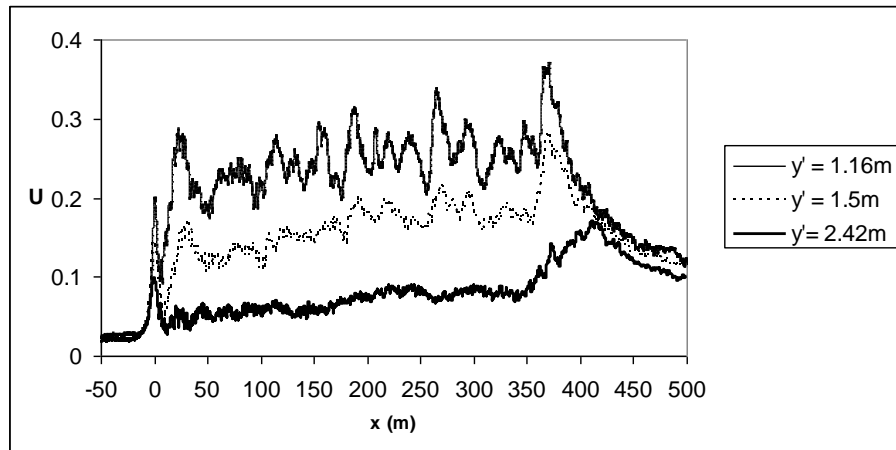


Figure 1 Ensemble averaged slipstream velocities from the RAPIDE experiments – Full scale experiments, 14 car ICE-1, measurements at trackside; y' =distance from nearest rail, height above track = 0.5m. Velocities normalised with train velocity, and x distance measured from nose of train. From [2].



a) The experimental site GY in Spain



b) The Westendorf platform and trackside sites



c) The Kutzenhausen platform site

Figure 2 The experimental sites

High speed single units



S-100



S-102



S-103



S-120



S-130



ICE-1



ICE-2



ICE-3



ICE-T

Low speed multiple unit



BR440

Locomotives plus coaches



S-252 loco plus coaches



Dosto BR111 loco leading



Dosto BR111 loco trailing



BR101 loco plus coaches



Class 91 loco plus coaches

Figure 3 The experimental trains

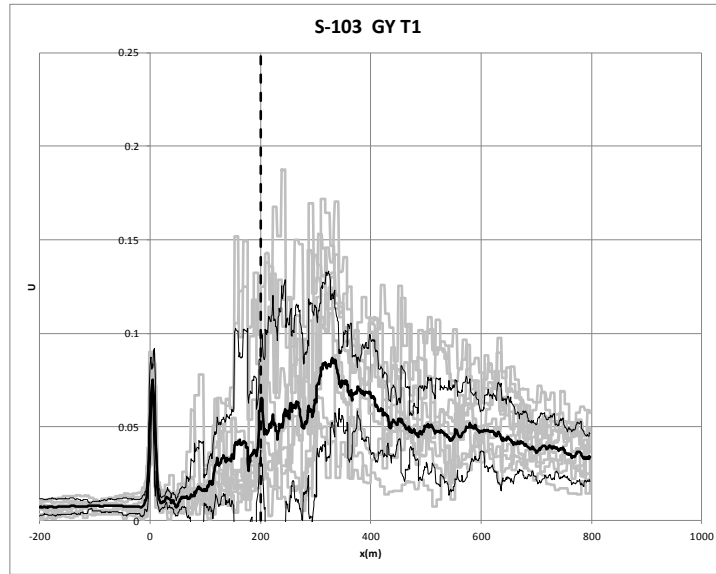


Figure 4 Individual runs and ensemble means and standard deviations for the S-103 (solid black line is the ensemble mean; lighter black lines are the mean \pm the standard deviation; the zero position on the x axis coincides with the front of the train; the vertical dashed line indicates the end of the train). The y axis shows the horizontal slipstream velocity normalised with train speed.

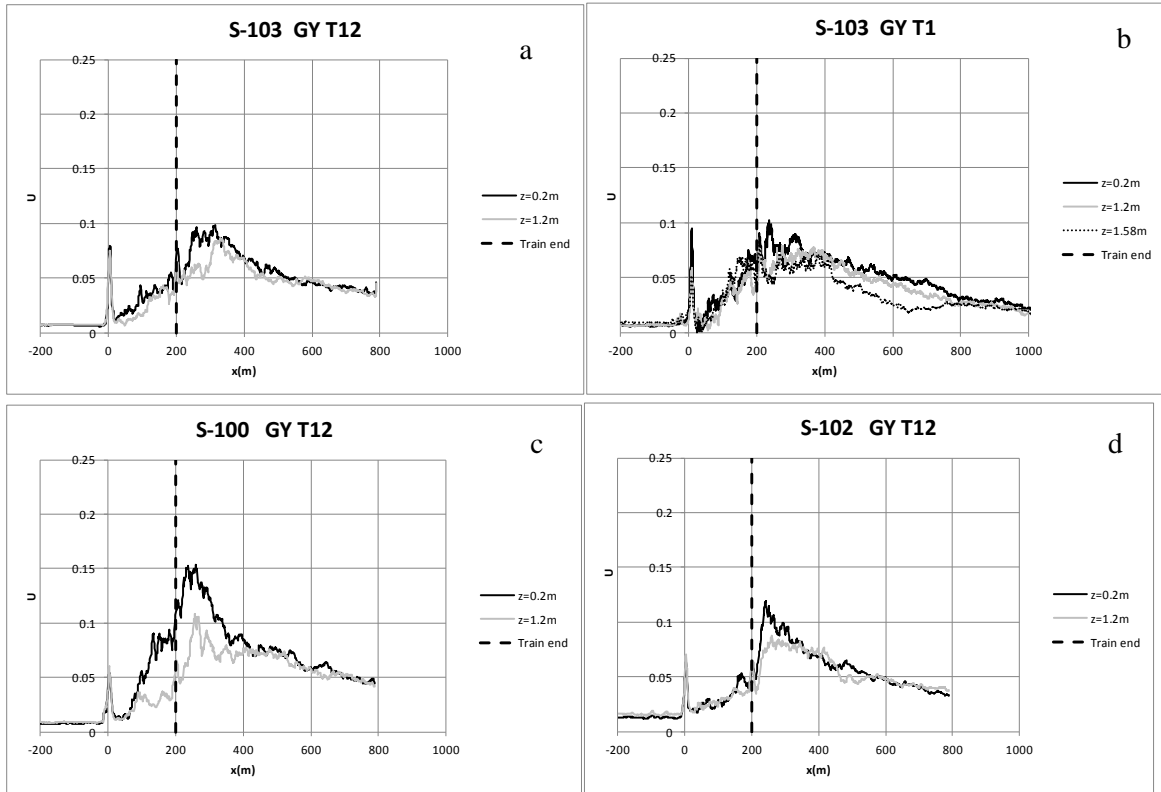


Figure 5 (continued over page)

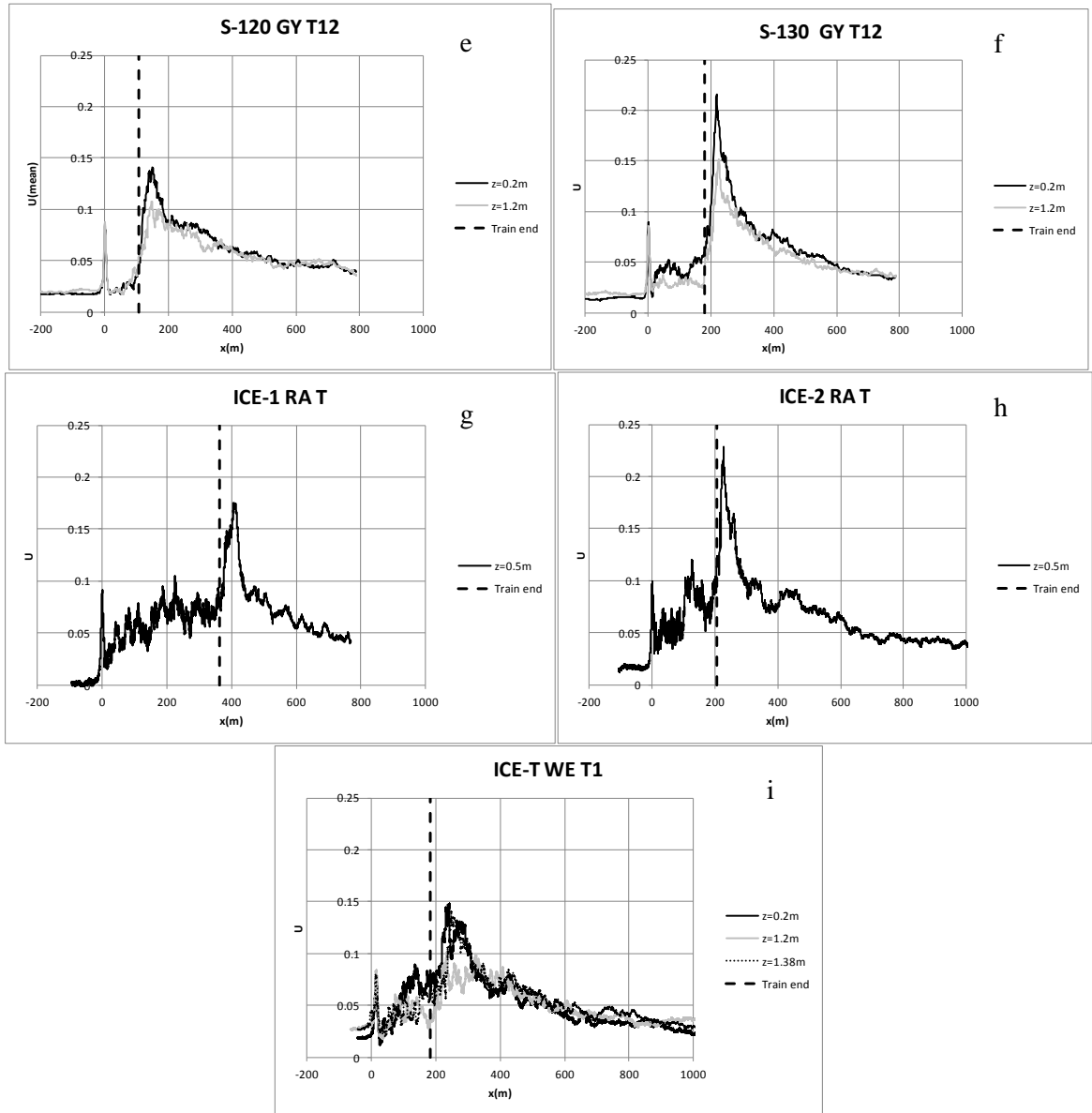


Figure 5 Ensemble averages for slipstream velocities for high speed single units, measured at the trackside

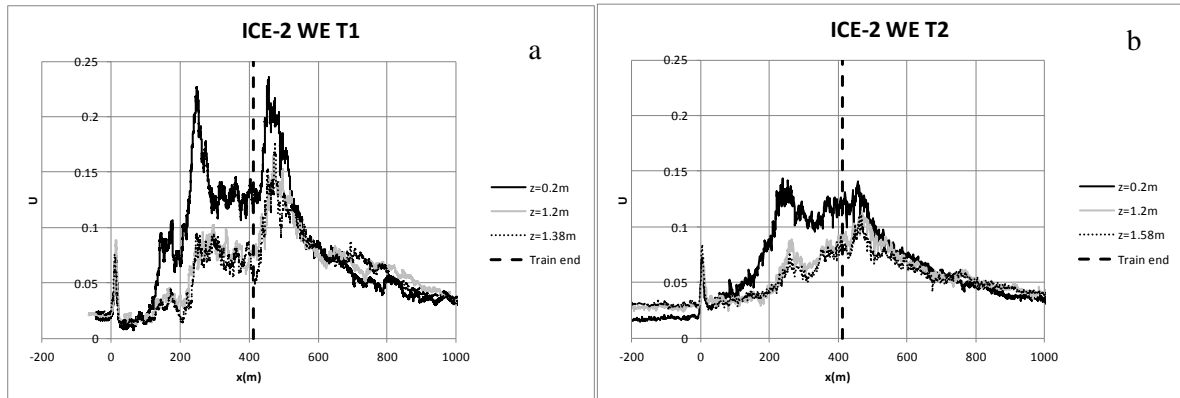


Figure 6 Ensemble averages for slipstream velocities for high speed double units, measured at the trackside

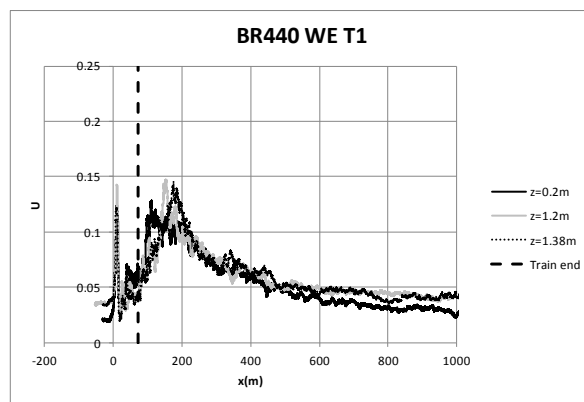


Figure 7 Ensemble averages for slipstream velocities for short passenger units, measured at the trackside

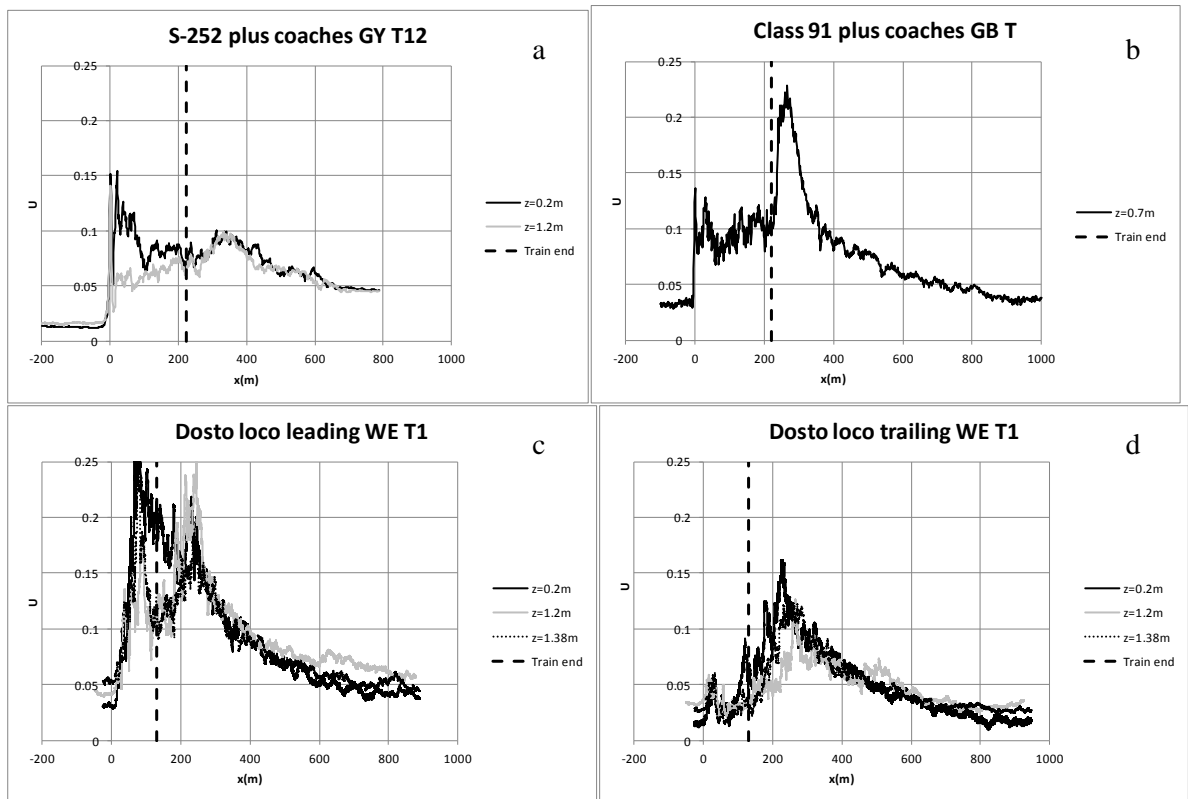


Figure 8 Ensemble averages for slipstream velocities for locomotives plus coaches, measured at the trackside

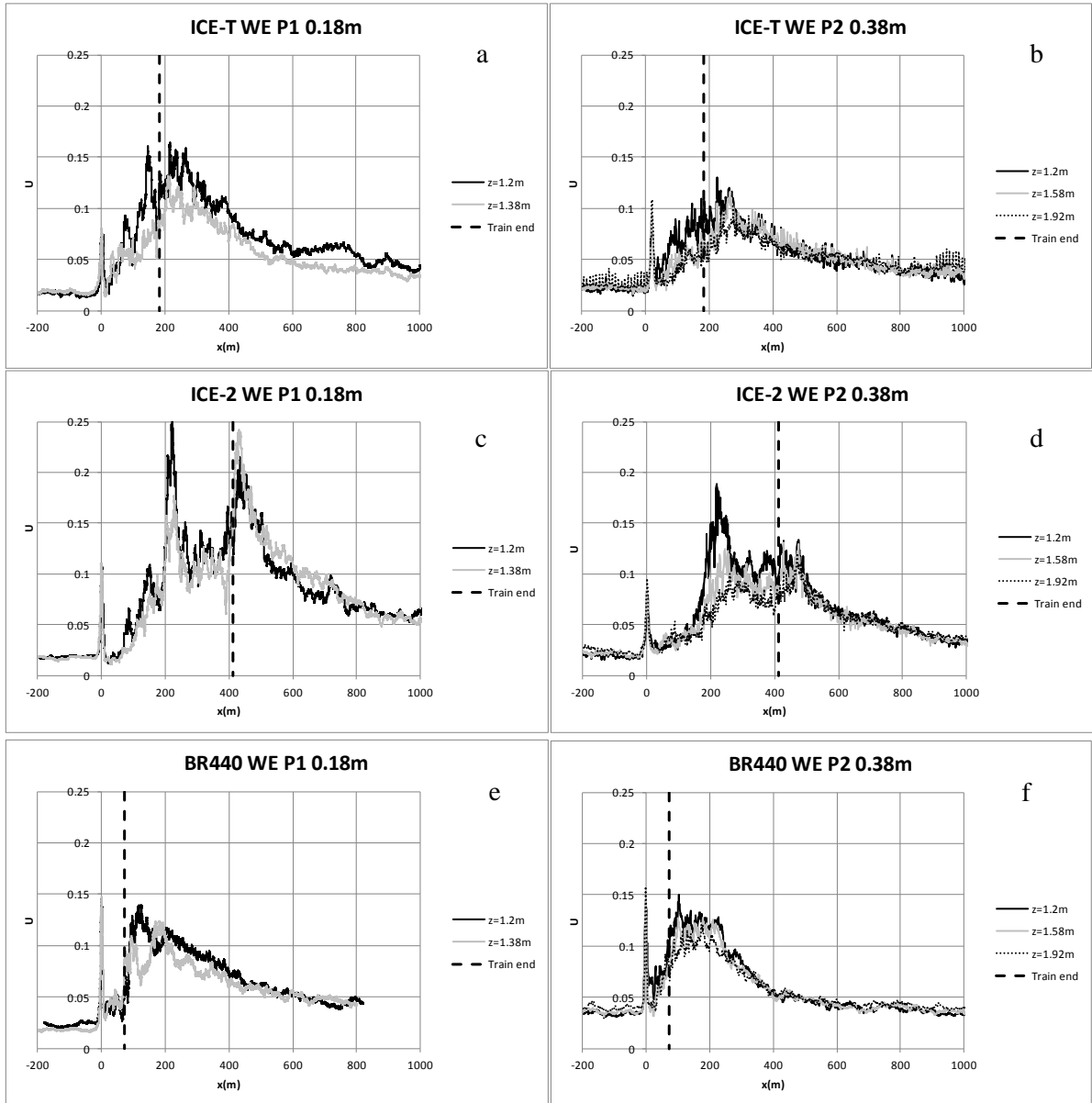


Figure 9 Comparison between ensembles on platforms of different heights

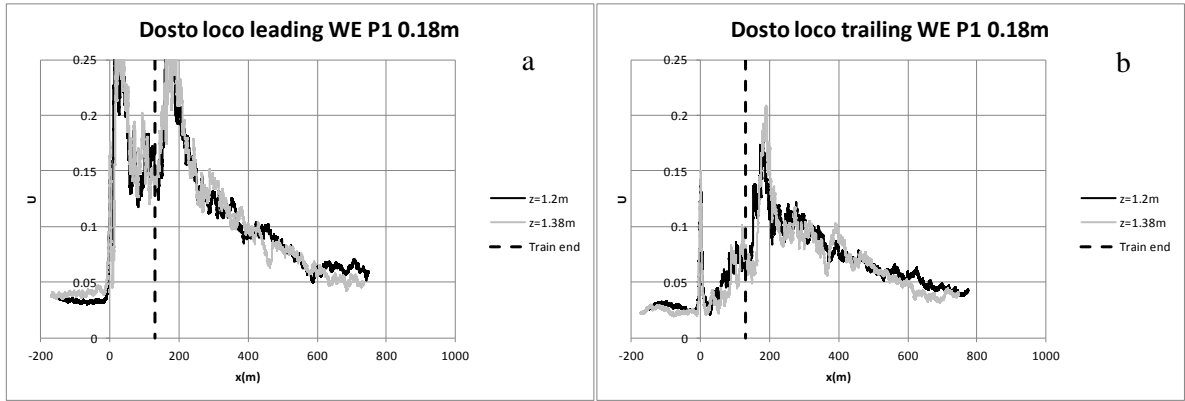


Figure 10 Ensemble mean slipstreams above a platform, for DOSTO with locomotive leading and trailing.

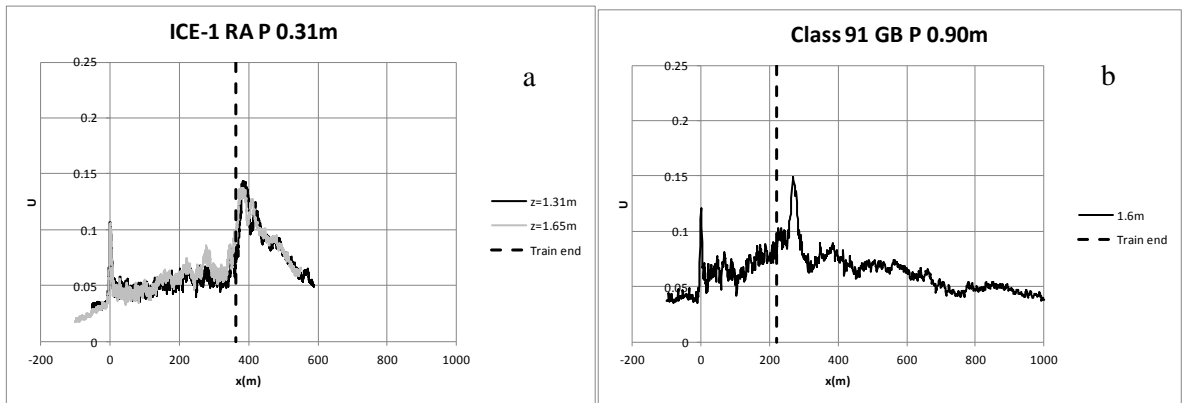


Figure 11 Ensemble mean slipstreams for ICE-1 and Class 90 plus coaches above platforms

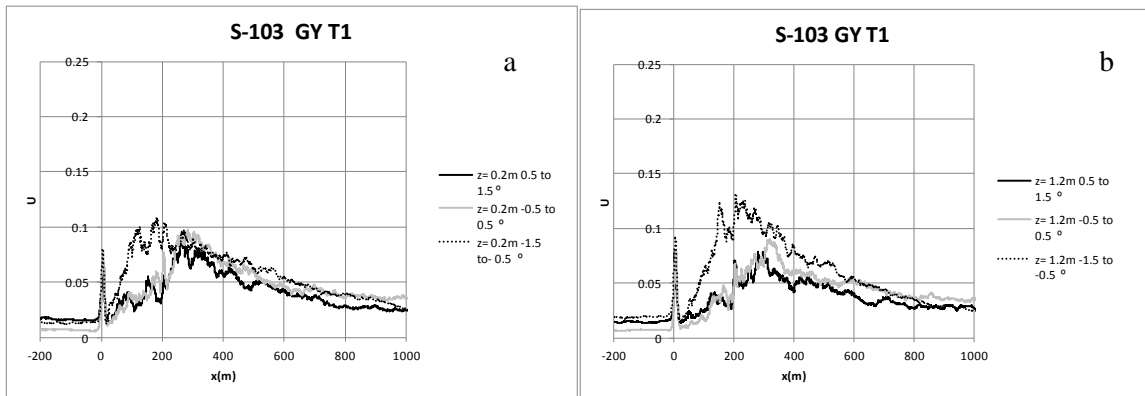


Figure 12. The effect of crosswinds

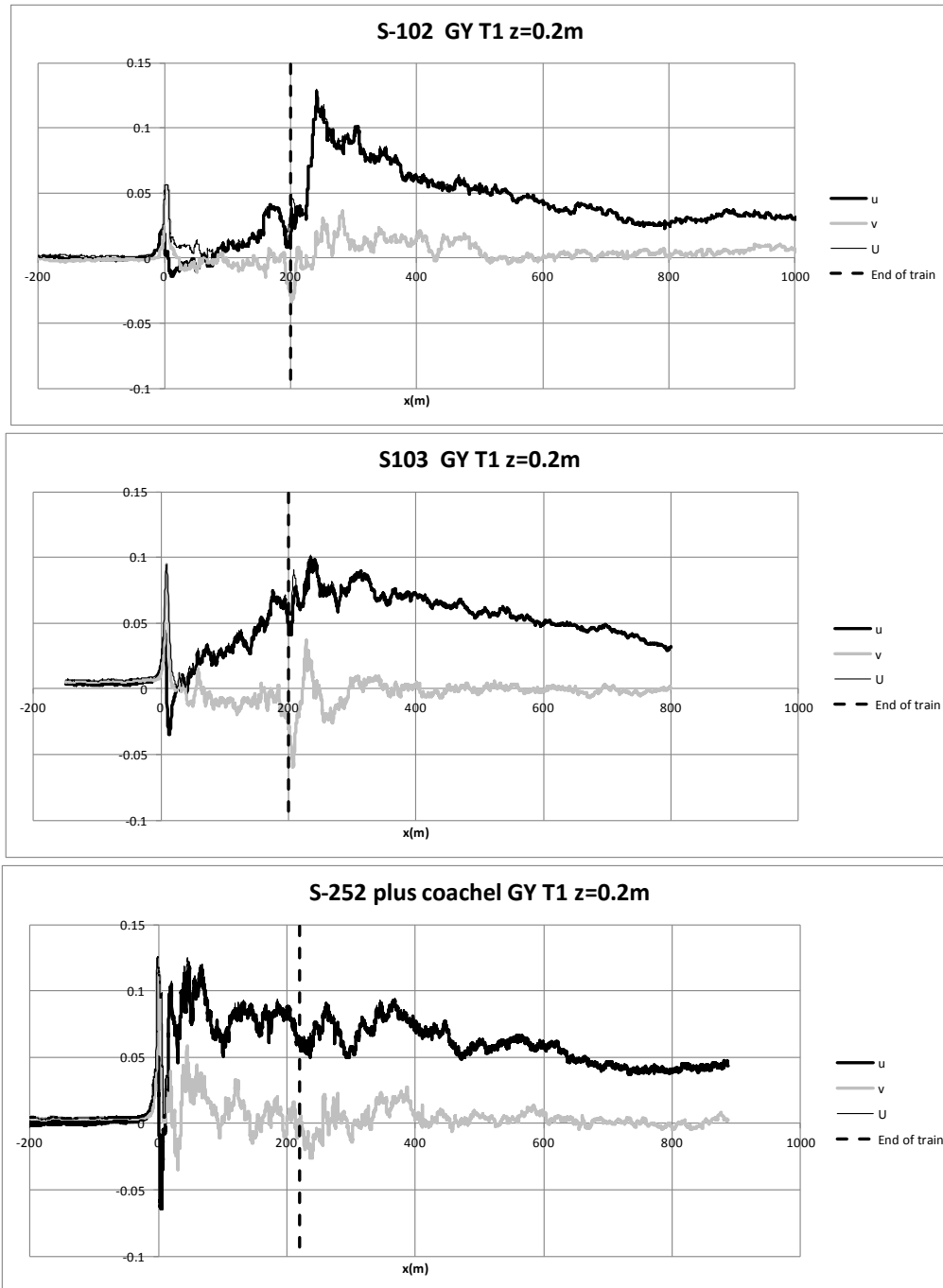


Figure 13 Ensemble averages of velocity components.

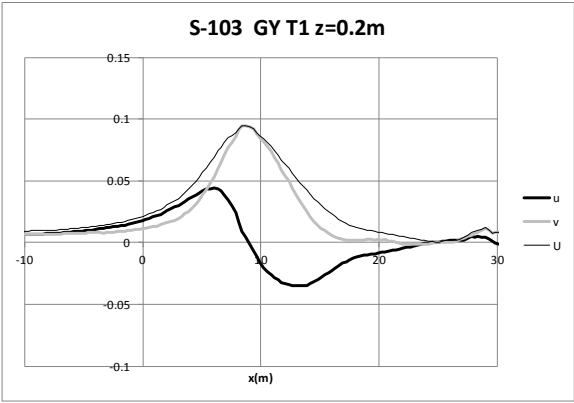


Figure 14 Expanded ensemble averages of velocity components for the S103 Velar nose peak.

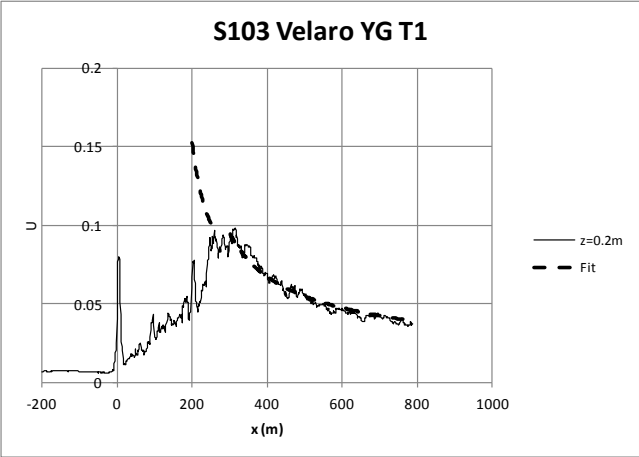


Figure 15 Power law curve fit for S103 Velaro far wake.

Sites or dataset (Notes 1,2,3)			GY T12	GY T1	WE T1	WE T2	WE P 1	WE P2	KH P	RA T	RA P	GB T	GB P	
Investigator (Note 4)			DB	BT	DB	UB	DB	UB	UB					
Anemometer heights above top of rail (m) (Notes 5,6,7,8)			0.2	0.2	0.2	0.2			0.76	0.5		0.7		
			1.2	1.2	1.2 1.38	1.2 1.58	1.2 1.38	1.2 1.58 1.92	1.2 1.58	1.2 1.38 1.58		1.31		1.6
Platform height (m)							0.18	0.38	0.38		0.31		0.9	
Train	Length (m)	Max speed (kph)												
High speed trains, single unit														
S-100	200	300	x	x										
S-102	200	300	x	x										
S-103	200	300	x	x										
S-120	107	250	x	x										
S-130	180	250	x	x										
ICE-1	364	280							x	x	x			
ICE-2	206	280								x				
ICE-3	400	320							x					
ICE-T	184	230			x	x	x	x						
High speed trains double unit														
S-102	400	300	x	x										
S-103	400	300	x	x										
ICE-2	411	280			x	x	x	x						
Low speed multiple unit														
BR440	71	160			x	x	x	x						
Locomotives and carriages														
S252 + coaches	222	200	x	x										
Dosto loco leading	130	140			x			x						
Dosto loco trailing	130	140			x			x						
EC101 + coaches	280	220							x					
C91 + coaches	220	225										x	x	

Notes

1. Sites. GY - Guadalajara – Yebes in Spain, WE – Westendorf in Germany, KH – Kutzenhausen in Germany
2. Datasets. RA – RAPIDE database, GB – GB database
3. T1 – track 1, T2- track 2, T12 – tracks 1 and 2, P1 – platform 1, P2 – platform 2, T – trackside, P – platform
4. Investigators. DB – Deutsche Bahn, BT – Bombardier Transportation, UB – University of Birmingham
5. All anemometers, except those mentioned below, were at 3.0m from the centre of the track i.e. the TSI measurement positions.
6. 1.92m WE P2 is based on GB positions, 2.5m from the nearest track (3.25m from track centreline).
7. RA T measurements were made 2.5m from the track centre line. RA P measurements were made 1.5m from platform edge, approximately 3.0m from track centreline
8. GB T measurements were made 1.95m from nearest rail

Table 1 The experimental sites, trains and measurement positions

Train	Speed range m/s	GY T12	GY T1	WE T1	WE T2	WE P 1	WE P 2	RA T	RA P	GB T	GB P
High speed trains single units											
S-100	79-86	16									
S-102	75-84	20									
S-103	79-80	20	20								
S-120	53-71	20									
S-130	44-66	20									
ICE-1	51-69							9	11		
ICE-2	60-78							7			
ICE-T	29-54			7	33	7	15				
High speed trains double units											
ICE-2	45-54			8	32	8	14				
Low speed passenger units											
BR440	20-47			10	49	11	20				
Locomotives and carriages											
S252 + coaches	45-56	20									
Dosto loco leading	32-39			9		9					
Dosto loco trailing	32-38			7		7					
C91 + coaches	44-63									8	8

Table 2 Number of train runs used in ensemble analysis

	$z(m)$	Length (m)	site	U(nose peak)	n
High speed single units					
S-100	0.2	200	GY T12	0.054	-0.50
	1.2		GY T12	0.051	-
S-102	0.2	200	GY T12	0.050	-0.55
	1.2		GY T12	0.054	-0.48
S-103	0.2	200	GY T12	0.073	-0.57
	1.2		GY T12	0.068	-0.50
S-120	0.2	107	GY T12	0.066	-0.48
	1.2		GY T12	0.067	-0.39
S-130	0.2	180	GY T12	0.075	-0.64
	1.2		GY T12	0.067	-0.56
Short passenger unit					
BR440	0.2	71	WE T1	0.103	-0.66
	1.2		WE T1	0.108	-0.46
	1.2		WE P1	0.120	-0.67
Locomotive coach combinations					
S-252 plus coaches	0.2	222	GY T12	0.140	-0.50
	1.2		GY T12	0.124	-0.50

Table 3 Nose peak and wake exponent values for different train types